A&A manuscript no.
(will be inserted by hand later)

Your thesaurus codes are:
11.05.2, 11.07.1, 11.09.2, 11.16.1, 11.16.2, 11.19.2

ASTRONOMY AND ASTROPHYSICS

Statistics of galaxy warps in the HDF North and South

V. Reshetnikov[1,5], E. Battaner[2], F. Combes[3], and J. Jiménez-Vicente[4]

[1] Astronomical Institute of St.Petersburg State University, 198504 St.Petersburg, Russia
[2] Depto. Física Teórica y del Cosmos, Universidad de Granada, Spain
[3] DEMIRM, Observatoire de Paris, 61 Av. de l'Observatoire, 75014 Paris, France
[4] Groningen Kapteyn Laboratorium, Groningen, Netherlands
[5] Isaac Newton Institute of Chile, St.Petersburg Branch

Received 6 September 2001; Accepted 13 November 2001

Abstract. We present a statistical study of the presence of galaxy warps in the Hubble deep fields. Among a complete sample of 45 edge-on galaxies above a diameter of $1.''3$, we find 5 galaxies to be certainly warped and 6 galaxies as good candidates. In addition, 4 galaxies reveal a characteristic U-warp. Compared to statistical studies of local warps, and taking into account the strong bias against observing the outer parts of galaxies at high redshift, these numbers point towards a very high frequency of warps at $z \sim 1$: almost all galaxy discs might be warped. Furthermore, the amplitude of warps are stronger than for local warps. This is easily interpreted in terms of higher galaxy interactions and matter accretion in the past. This result supports these two mechanisms as the best candidates for the origin of early warps. The mean observed axis ratio of our sample of edge-on galaxies is significantly larger in the high-z sample than is found for samples of local spiral galaxies. This might be due to disk thickening due to more frequent galaxy interactions.

1. Introduction

Warping of outer galactic disks is a very common phenomenon, with amplitude increasing with radius. Warps are mostly conspicuous in the HI plane, since the atomic gas extends up to 100kpc, and its radius is often several times that of the optical disk (e.g. Bosma 1978, Briggs 1990). However warps start at the outskirts of optical disks, and careful investigation of edge-on galaxies have revealed that a significant percentage (40-50%) of stellar disks are also warped (Sánchez-Saavedra et al. 1990, Reshetnikov & Combes 1998).

The origin of warps has been a puzzle for a long time, since orbits slightly inclined with respect to the plane precess around the disk rotation axis, and the precession is differential: the life-time of warps would be much less than the Hubble time. Several mechanisms to trigger and maintain warps have been proposed, including tidal interactions between galaxies, inter-galactic magnetic fields, disk-halo interaction and matter accretion (see the review by Binney, 1992). The forcing of a misaligned halo does not appear to be a promising solution, since the halo and disks align over a short time-scale (Nelson & Tremaine 1995, Binney et al. 1998). On the contrary, galaxy interactions have been revived as an explanation, since even the prototypical isolated warped galaxy NGC 5907 has been found to interact with small companions (Shang et al. 1998). The other likely alternative is gas accretion, since it has been realized that galaxies are still significantly growing in mass during all their lives, and are surrounded by a network of filaments accounting for the Lyman-α absorbers (e.g. Davé et al. 1999). The outer parts of galaxies could be constantly accreting gas at an inclined angular momentum, explaining the persistence of warps. The dark matter is also constantly raining down onto the dark galactic halo, with a skewed angular momemtum, making the galaxy reorient completely in a few Gyrs (Jiang & Binney 1999).

If these two mechanisms, matter accretion and tidal interaction with companions, are the main drivers of warps, it is very likely that warps were even stronger and more frequent in the past. Knowing this frequency at high redshift would help to discriminate between models of the warp origin. We thus undertake such an investigation in the Hubble Deep Fields. The main goal of our work is to study the frequency of optical warps at $z \sim 1$. At present, HI-21cm observations are not sensitive enough (and have insufficient spatial resolution) to probe high redshift galaxies.

Throughout this paper, we adopt a flat cosmology with $q_0 = 0.5$ and $H_0 = 70\ \mathrm{km\,s^{-1}\,Mpc^{-1}}$. If not differently specified, magnitudes are expressed in the AB system (Oke 1974).

2. The sample

The Hubble deep fields north and south (HDF-N and HDF-S, respectively) are the best available sources of data on the distant Universe (see Ferguson et al. 2000 for a comprehensive review). The two fields give the possibility to study distant field galaxies to the faintest levels currently

Send offprint requests to: V.P. Reshetnikov resh@astro.spbu.ru

achievable. Therefore, we selected HDF-N and HDF-S to study optical warps in remote galaxies.

2.1. Selection

We select our sample of distant edge-on galaxies on the basis of visual inspection of original HDF-N and HDF-S frames in the F814W filter (hereafter I_{814}). Visual selection is probably the best way to recognize true strongly inclined spirals among a huge number of asymmetric and peculiar objects in the two crowded deep fields.

The resulting sample of selected objects consisted of 50 edge-on galaxies. Tables 1 and 2 summarize the main characteristics of the galaxies.

The columns of Table 1 are: number according to the catalogue of Fernández-Soto et al. (1999); coordinates (in pixels); Williams et al. (1996) identification; I_{814} magnitude in the *AB* photometric system; spectroscopic redshift (Cohen et al. 2000; Hogg et al. 2000); photometric redshift (Fernández-Soto et al. 1999); photometric redshift according to Fontana et al. (2000); best-fit spectral type of galaxy (Fernández-Soto et al. 1999); index of warp (see sect.3.2).

The columns of Table 2 are: the name according to the Stony Brook catalogue (Fernández-Soto al. 1999) (the numbers mean coordinates in pixels); I_{814} magnitude in the *AB* photometric system; photometric redshift (Fernández-Soto et al. 1999); photometric redshift according to Fontana et al. (2000); best-fit spectral type of galaxy (Fernández-Soto et al., 1999); index of warp.

2.2. Completeness

Visual classification is possible for relatively large galaxies only. Thus one can expect that our sample is a diameter-limited sample. In order to estimate the completeness limit we applied the well-known V/V_{max} test (Schmidt 1968). For a diameter-limited sample the ratio between the volume of the sphere determined by the object distance (V) and the maximum volume of the sphere in which the object could lie and still have been included in the sample (V_{max}) is $V/V_{max}=(d_0/d)^3$, where d is the apparent angular diameter of the galaxy and d_0 is the minimum diameter of the sample selection criterion (e.g. Thuan & Seitzer 1979). For objects distributed uniformly in space the average value of V/V_{max} should be $0.5\pm1/\sqrt{12\times N}$, where N is the number of sample galaxies.

We determined the apparent major axis angular diameter (d) within the isophote $\mu(I_{814}) = 26.0$ for all the sample galaxies. Then, changing d_0 and computing the V/V_{max} ratio, we found that for $d_0=1.''33$ $\langle V/V_{max}\rangle=0.50\pm0.04$. Therefore, our sample is nearly complete for the galaxies with diameter $d>1.''3$. (Note that we used the isophotal sizes of galaxies for the V/V_{max} test. This is not quite correct due to the influence of the cosmological dimming and K–correction on the apparent sizes of galaxies. Note also that surface brightness evolution – e.g. Lilly et al. 1998 – must partially compensate the above mentioned effects.)

Only five galaxies (n112, n246 in the HDF-N and s0932, s2504, s2816 in the HDF-S) show major axis diameters smaller than $1.''3$. We will consider the rest of the sample – 45 galaxies – as a complete sample.

2.3. General characteristics

Fig.1 shows the distribution of the selected objects within the HDF-N and HDF-S. Uniform angular distribution of galaxies is evident in the figure. HDF-N contains more edge-on galaxies (32) than HDF-S (18). This difference probably reflects the general excess of galaxies in the northern field at $z \leq 1$ (Gwyn 1999).

We present available spectroscopic and photometric redshifts of the galaxies in tables 1 and 2. Unfortunately, we have spectroscopic redshifts for only about half of the objects (14) in the HDF-N. For the remaining galaxies we will use the mean photometric redshifts from the catalogues of Fernández-Soto et al. (1999) and Fontana et al. (2000). The edge-on orientation and, therefore, strong internal absorption can distort the observed spectral energy distribution of a galaxy and can introduce some systematic effects in the derived photometric redshift. To check for this possible effect, we compared two catalogues of photometric redshifts with spectroscopic data. The two sets of photometric redshifts demonstrate relatively good agreement (Fig.2):
$\langle z_{fsoto} - z_{font}\rangle = +0.00 \pm 0.31(\sigma)$ (N=50) or
$\langle z_{fsoto} - z_{font}\rangle = +0.05 \pm 0.13$ ($z \leq 1.8$, N=46).
The comparison of spectroscopic and photometric redshifts does not show any systematic effects (Fig.2):
$\langle z - z_{fsoto}\rangle = +0.02 \pm 0.26$ (N=14),
$\langle z - z_{font}\rangle = -0.03 \pm 0.31$ (N=14).
The largest differences between photometric and spectroscopic z are for n716 and n727. These two galaxies are very close in projection ($2.''9$ or 17 kpc at $z = 0.92$) and show close spectroscopic z (see table 1). We suppose that these galaxies form a real physical pair and that their spectral energy distributions are strongly distorted by tidally-induced star formation.

Fig.3 presents the redshift distribution of edge-on galaxies. The distribution is peaked at $z \sim 0.8 - 0.9$ (table 3) and is located in the low-redshift wing of a global redshift distribution of galaxies in the deep fields (bottom part of Fig.3). This is probably explained by our diameter-limited selection of the sample.

Fig.4 shows the distribution of apparent axial ratios – b/a – of the sample objects. The b/a values were estimated from the ellipse-fitting of outer contours of the galaxies. Our b/a estimates are very close to those published in the Williams et al. (1996) catalogue. The mean ratio $\frac{b/a(\text{pres.work})}{b/a(\text{Williams})}$ is $1.01\pm0.21(\sigma)$. The average value of axial ratio – 0.32 (table 3) – significantly exceeds the b/a

Table 1. Edge-on galaxies in the HDF-N

N	Mosaic (X,Y)	Williams et al. (1996) ID	I_{814}	z	z_{fsoto}	z_{font}	Type	Warp
15	733.9,271.3	3-923.0	24.70		0.40	0.49	Scd	6
16	1342.8,274.7	3-925.0	24.93		0.92	0.88	Irr	U
55	3893.6,380.4	4-976.2	23.32		0.20	0.15	Irr	
81	3232.6,433.0	4-618.0	23.94		0.64	0.60	Irr	
112	2764.7,508.1	4-386.0	26.09		1.08	0.87	Irr	
120	1368.7,534.7	3-786.0	24.27		1.60	1.60	Irr	
153	673.6,598.0	3-761.1	24.94		0.76	0.69	Irr	
246	2154.6,809.8	4-70.0	26.99		1.48	1.69	Irr	
273	2107.1,872.3	4-33.0	22.47	0.905	0.68	0.80	Ell	
304	1747.1,951.1	3-593.1	25.60		1.760	1.79	Scd	U
319	2178.7,989.2	4-85.1	24.41	0.961	0.92	0.90	Irr	U
450	929.2,1329.3	3-398.1	24.25		0.72	0.67	Irr	
476	2430.9,1390.5	4-232.12	22.77	0.421	0.48	0.45	Irr	
506	1899.5,1472.4	3-331.0	24.47	0.751	1.08	0.75	Irr	
534	3812.9,1545.4	4-926.1	23.82		1.04	0.85	Sbc	5
632	3483.8,1771.9	4-745.0	25.80		1.60	1.88	Irr	
671	2166.4,1877.4	4-89.0	23.93	0.681	0.76	0.65	Irr	
716	3849.0,2034.0	4-946.0	22.61	0.944	0.68	0.45	Sbc	5
727	3792.2,2078.6	4-916.0	23.93	0.904	0.16	1.88	Scd	6
733	3628.1,2104.3	4-829.1	25.04		0.96	0.91	Irr	
749	1458.6,2208.5	2-339.1	22.60	0.851	0.88	0.95	Sbc	U
774	2521.0,2361.5	1-34.1	21.22	0.485	0.68	0.40	Sbc	
805	172.2,2492.4	2-1022.0	25.33		0.72	0.59	Irr	
817	2793.4,2550.5	1-57.11111	22.19	0.485	0.68	0.50	Sbc	4
886	1835.2,2838.4	2-133.0	25.25		1.00	0.94	Irr	
888	196.0,2852.5	2-1018.0	23.70	0.559	0.64	0.56	Irr	
898	1958.2,2909.9	2-65.1	25.89		0.92	0.95	Irr	6
899	181.2,2923.1	2-1023.1	22.94	0.564	0.68	0.60	Scd	
938	765.0,3128.9	2-702.1	23.03	0.557	0.52	0.55	Scd	
979	327.1,3397.0	2-950.0	23.45	0.517	0.44	0.50	Scd	4
1027	1230.6,3650.7	2-432.0	23.88		0.92	0.87	Irr	
1031	1590.7,3680.9	2-270.2	25.08		1.20	0.93	Scd	

Table 2. Edge-on galaxies in the HDF-S

Name	I_{814}	z_{fsoto}	z_{font}	Type	Warp
SB-WF-0501-0760	25.07	1.11	1.31	Irr	
SB-WF-0564-0515	25.27	1.01	1.03	Irr	
SB-WF-0566-1028	25.67	1.79	2.52	Scd	
SB-WF-0578-2216	23.16	1.08	0.88	Scd	6
SB-WF-0747-1929	25.31	1.07	0.88	Irr	
SB-WF-0932-2115	25.58	1.03	0.88	Scd	
SB-WF-1085-0562	25.51	1.07	1.19	Irr	
SB-WF-1404-2925	23.09	0.54	0.45	Sbc	
SB-WF-2340-1898	24.21	0.55	0.56	Irr	
SB-WF-2353-1914	24.36	0.30	0.31	Scd	
SB-WF-2504-3117	24.80	1.20	1.09	Irr	4
SB-WF-2661-4090	24.10	0.92	0.92	Irr	
SB-WF-2691-2966	25.05	0.49	0.42	Irr	
SB-WF-2816-2895	26.04	0.47	0.63	SB1	
SB-WF-3053-1963	26.07	1.18	0.91	Scd	5
SB-WF-3329-2173	24.54	0.27	0.32	Scd	
SB-WF-3458-1026	23.40	0.69	0.69	Scd	6
SB-WF-3685-2040	26.63	2.43	2.03	SB1	

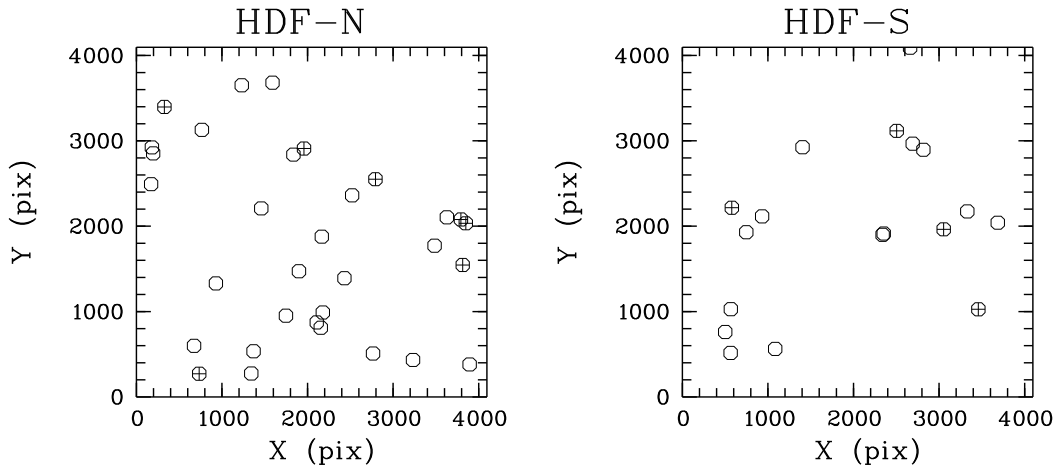

Fig. 1. Distribution of edge-on galaxies within the two fields. Crossed circles – galaxies with possible warps (see tables 1 and 2).

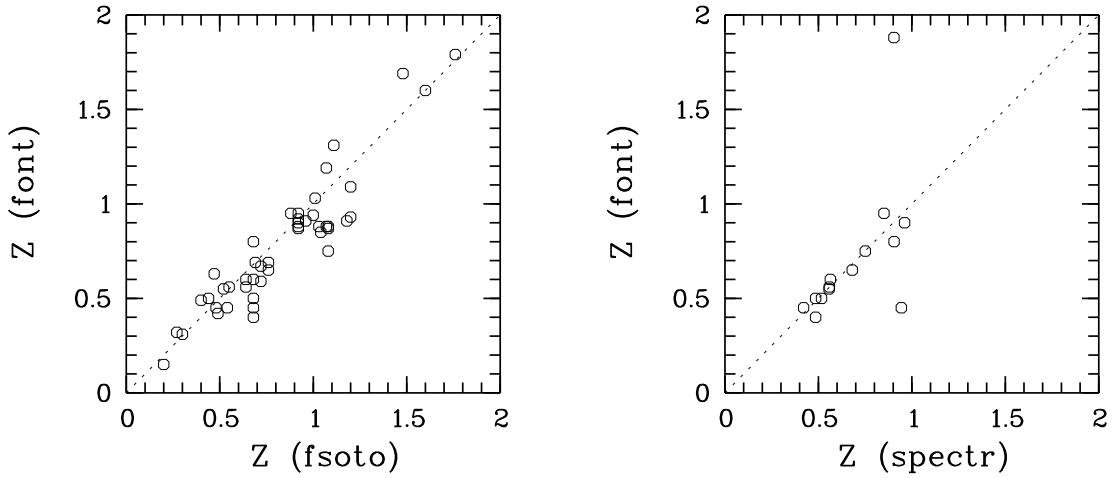

Fig. 2. Left: comparison of photometric redshifts of our sample edge-on galaxies according to Fernández-Soto et al. (1999) and Fontana et al. (2000) catalogues. Right: comparison of spectroscopic and photometric redshifts for 14 edge-on galaxies.

ratio for local spiral galaxies. According to Guthrie (1992) the true axial ratio of spiral disks is only 0.11–0.13. Assuming a very conservative true axial ratio of our sample of edge-on galaxies $b/a = 0.2$, we can estimate that the observational value (0.32) corresponds to a rather large inclination of the galaxies ($i \sim 75^{\rm o}$). Such a large departure from edge-on orientation must lead to very strong asymmetry of the surface brightness distributions along the minor axis. However we do not see any such significant asymmetries among the sample galaxies. Another possible reason is that the sample objects possess a large intrinsic axial ratio ($b/a \approx 0.3$) – about twice that of local spirals. This conclusion is consistent with the facts that 1) interaction and merger rates were significantly higher in the past (see Le Févre et al. 2000, Reshetnikov 2000 and references therein) and 2) galaxy interactions lead to thickening of the stellar disks (Reshetnikov & Combes 1997; Schwarzkopf & Dettmar 2000; see also Karachentsev & Karachentseva 1974). Of course, our conclusion is extremely tentative since we must check possible influence of the PSF on the observed thicknesses of edge-on galaxies in the HDF.

The mean *isophotal* diameter of the sample galaxies within $\mu(I_{814}) = 26.0$ is $2.''15 \pm 0.''9$ or 12.9 kpc at $z = 0.9$.

The rest-frame absolute magnitudes in the B passband were estimated following Lilly et al. (1995):
$M(B) = I_{814} - 5\log(D_L/10\,{\rm pc}) + 2.5\log(1+z) + (B - I_{814,z})$, where D_L is the luminosity distance and $B - I_{814,z}$ is the K-correction color. For our purposes we used the $B - I_{814,z}$ term for Irr galaxy (Lilly et al. 1995). At

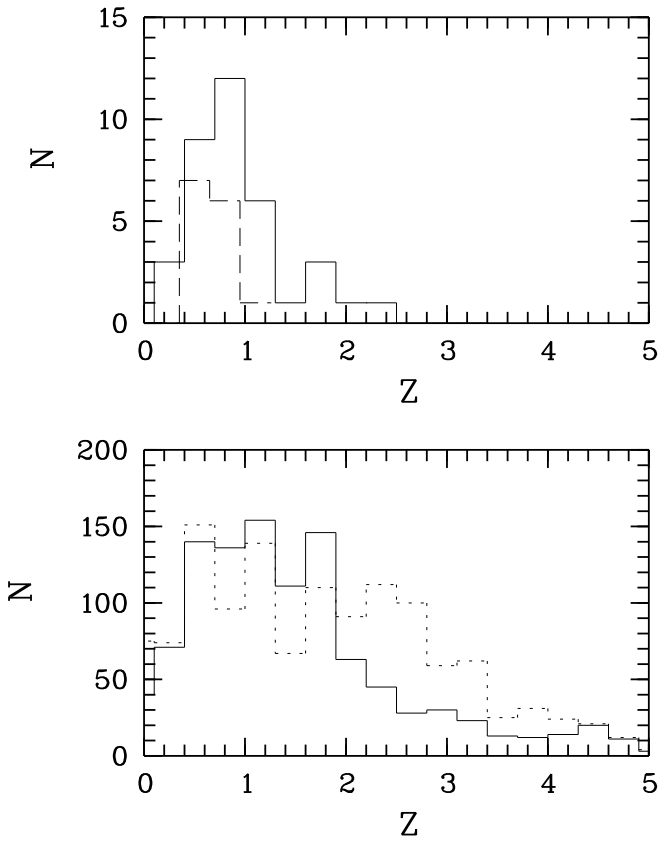

Fig. 3. Top: redshift distribution of edge-on galaxies (solid line shows galaxies with photometric redshifts, dashed line – with spectroscopic determinations). Bottom: distributions of the photometric redshifts in the HDF-N (solid line) and HDF-S (dashed line) according to Fernández-Soto et al. (1999) and Fontana et al. (2000) catalogues.

Table 3. Mean characteristics of the sample

Parameter	HDF-N	HDF-S	N+S
Number	32	18	50
$\langle I_{814}\rangle$	24.15±1.30(σ)	24.88±1.02	24.41±1.24
$\langle z\rangle$	0.85±0.38	0.95±0.54	0.89±0.44
$\langle b/a\rangle$	0.31±0.07	0.34±0.08	0.32±0.08
$\langle M_B\rangle$	–18.1±1.2	–17.7±1.4	–17.9±1.3

high redshifts, this term is small since I_{814} is redshifted down toward the rest-frame B filter (they coincide at $z = 0.83$). The resulting mean rest-frame absolute magnitude is $M(B) \approx -18$ (table 3). After correction for internal absorption the absolute magnitude must be ≈ -19. Therefore, our sample objects are sub-L^* galaxies.

The mean parameters of the sample are summarized in table 3.

3. Statistics of warped galaxies

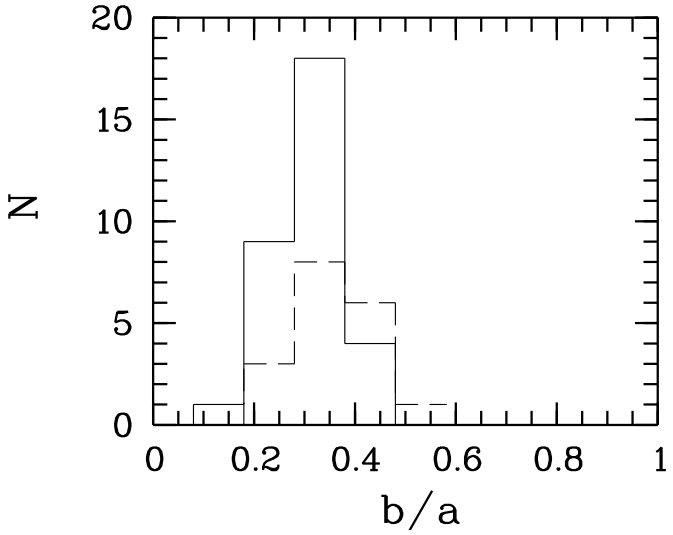

Fig. 4. Apparent axial ratios: HDF-N (solid line) and HDF-S (dashed line).

3.1. Could we recognize local warps at high redshifts?

Searching for optical warps in the disks of distant galaxies is a difficult enterprise. In local galaxies optical warps become detectable in the outer parts of their disks. For instance, from a sample of 45 spirals with measureable warps, Reshetnikov (1995) estimated that the average value of the surface brightness level at which optical warping becomes detectable is $\mu(R) = 23.0\pm0.8$ (in the Cousins R passband) or $\mu(B) \approx 24$. (After correction for the line-of-sight integration, this level corresponds to $\mu(B) \approx 25$ for face-on galaxy.) Moving such a typical object at $z = 0.9$ (average redshift of our sample), this level will fall to $\mu(I_{814}) \approx 26$ (see Lilly et al. 1995 and note that the K-correction term is close to zero at this redshift). This surface brightness corresponds to $\sim 1.5\sigma$ limiting isophote of the deep fields and, therefore, we cannot recognize such a typical optical warp at $z \sim 1$.

In order to directly illustrate this conclusion we have redshifted the B band image of the local Sb spiral ESO 235-G53, which has a remarkable optical warp. The image of the galaxy was taken by R. de Grijs with the Danish 1.54-m telescope at La Silla, Chile, in July 1994. The prominent warp starts at the radius $\approx (1.2 - 1.7)h$ and reaches $\approx 10^o$ near the end of the disk (de Grijs 1997). Using the method described in Giavalisco et al. (1996), we placed ESO 235-G53 at $z = 0.83$ where redshifted B corresponds to I_{814}. The result of the redshifting is shown in Fig.5. (Note that this is just an illustrative figure and we faded the whole image including the foreground stars.) The result demonstrates that even such a strong warp cannot be detected.

We can conclude from the above exercise that among distant galaxies we can recognize only extremely strong and bright optical warps. Any statistics of warps in the

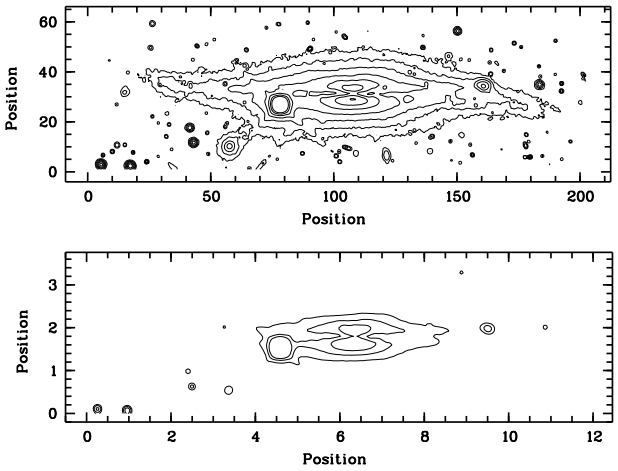

Fig. 5. Top: contour map of ESO 235-G53 in the B passband. The faintest contour corresponds to $\mu(B) = 27.0$. Bottom: contour map of the same galaxy moved at $z = 0.83$. The faintest contour corresponds to $\mu(I_{814}) = 26.5$ or $\sim 1\sigma$ limiting isophote of the HDF. Isophote step is $0.^m75$. Both axes are in arcseconds.

deep fields will give a strict lower limit of the true fraction due to a huge observational bias against finding them.

3.2. Selection of warped galaxies

The original I_{814}-band images and contour maps of all the sample galaxies were examined independently by three of us (E.B., F.C. and V.R.). On the basis of eyeball classification, they assigned an "index of warp" (IW) for each object: 0 – no warp, 2 – a certain integral-shaped warp, and 1 – intermediate case. We also marked U-shaped warps, when the plane bends towards the same direction on both sides (Reshetnikov & Combes 1998) like the letter "U". Then, we summed the personal indices for each object and decided to consider those galaxies with total IW=6 (index 2 for each observer) as true warps and IW=4-5 as good candidates for warped disks. There are 5 galaxies with true warps, and 6 good candidates in our sample of 50. Our classification for the galaxies with IW≥4 is presented in the last columns of tables 1 and 2. Contour maps of all galaxies with certain or possible warps are displayed in Fig.6 and 7. Note that these are just illustrative contour maps and they do not give the best impression of possible warps. A detailed inspection must be made on the original pictures.

These 11 galaxies were processed with a special software, written to automatically detect and measure some quantitative characteristics of warps. The software works essentially as the WIG program described by Jiménez-Vicente et al. (1997). First the images are rotated so the galaxies are roughly in a horizontal position and the pixels with a S/N>3 are selected. Then the warp curve (mean deviation from the equatorial plane for each radius) is calculated by fitting a gaussian to each column. Outliers are removed using S/N and continuity criteria. The flat part of the galaxy is defined by the average position angle of the inner FWHM of the galaxy disk.

Table 4. Characteristics of optical warps

Galaxy	ψ (°)	R_{warp} (arcsec)	R_{warp}/h
n15	4.5	0.58	1.5
n716	1.7	0.62	1.0:
n727	5.5	0.60	1.5
n817	5.3	0.88	1.8
n898	5.6	0.52	1.1:
n979	5.7	0.62	1.9
s0578	11.4	1.08	1.6:
s3053	9.2	0.66	1.2:
s3458	4.5	0.38	1.0:

The software detects a warp if there are more than five consecutive pixels with deviations larger than twice the standard deviation in the flat part. In this case the first of those pixels is taken as the starting radius of the warp. Then, the warp angle is determined for both sides (defined as the angle between the equatorial plane and the line joining the center with the point with the largest deviation from the equatorial plane in the warp curve) and averaged to give the average warp angle.

As a result, we confirmed that 9 of 11 galaxies demonstrate integral-like shapes according to our criteria.

Table 4 summarizes the general characteristics of optical warps in the sample according to the software. The columns are as follows: ψ – mean warp angle, R_{warp} – starting point of the warp, and R_{warp}/h – starting point of the warp to exponential scalelength ratio (uncertain values are marked by colons).

3.3. Statistics of warps

The measured mean warp angle is $\langle\psi\rangle = 5.^o9 \pm 2.^o8(\sigma)$ or, excluding two extreme cases (n716 and s0578), $5.^o8 \pm 1.^o6$. This value is larger than reported by Reshetnikov (1995) or Reshetnikov & Combes (1998) – 3°–4° – for local spirals. The mean warp angle for distant objects is also larger than for local galaxies with strongest optical warps – $4.^o8 \pm 1.^o3$ (Reshetnikov & Combes 1999).

The observed fraction of optical warps in the HDF-N and HDF-S is $9/50 = 0.18 \pm 0.06$ (Poisson error). Considering the "complete" sample of 45 galaxies, this fraction is $9/45 = 0.20 \pm 0.07$. The observed fraction is certainly an underestimate of the true fraction (see sect.3.1).

There is a possibility of confusing a warped disk with a slightly inclined (from edge-on) disk with a contrasted 2-spiral pattern (see the simulations in Reshetnikov & Combes 1998). This type of confusion should be less important at high redshift, since grand-design spirals appear

to be rarer for z≥0.3 or even absent in the past (cf van den Bergh et al. 2000). Possible projection of small background objects, for instance for n898 and s0578, can be rejected on the basis of smoothness and symmetry of the warp curves. However it is possible that in both cases we observe accretion of small companions by a large spiral galaxy.

To obtain a rough estimate of the true fraction of distant warps, let us assume that warped disks at $z \sim 1$ obey the same distribution of warp angles as the $z = 0$ spirals – ψ^{-5} (Reshetnikov & Combes 1998, 1999). Excluding two extreme cases with $\psi = 1.^\circ7$ and $11.^\circ4$, we have 7 galaxies with $\psi = 4.^\circ5 - 9.^\circ2$. Assuming that we selected all spirals in the two deep fields with $\psi = 4.^\circ5 - 9.^\circ2$, one can infer that the true number of galaxies with $\psi \geq 2.^\circ5$ must be 31 or ∼2/3 of all galaxies ($2.^\circ0$–$2.^\circ5$ is the detection limit of optical warps in our survey of local spirals – Reshetnikov & Combes 1998). Therefore, the actual fraction of warped disks at $z \sim 1$ is the same or even larger than at $z = 0$. Given the geometrical factor (warps along the line of sight are not detected), practically all distant disks are warped.

To draw a clearer conclusion about possible warp evolution with redshift, let us compare the frequencies of strongly warped disks at $z = 0$ and in the deep fields. In the two fields we found 8 galaxies with $\psi \geq 4.^\circ5$ (table 4). What is the equivalent fraction in the local universe? About 40% of spiral galaxies at $z = 0$ reveal S-shaped optical warps with $\psi \geq 2^\circ$ (Reshetnikov & Combes 1998). Adopting the ψ^{-5} law, one can estimate that the local frequency of spirals with $\psi \geq 4.^\circ5$ is 0.7%. Then, using the method described in Reshetnikov (2000), we found that the volume density of strong warps changes $\propto (1 + z)^m$ with $m = 3.8$. Assuming Poisson errors for galaxy numbers, we have $m = 3.8^{+0.6}_{-1.0}$ (owing to the uncertainty in the local frequency of strong warps, the actual error on m may be larger.) Comparing frequencies of galaxies with $\psi \geq 5.^\circ0$, we obtain $m = 4.0^{+0.8}_{-1.5}$. Our data therefore demonstrate a fast evolution of the volume frequency of *strong* optical warps at $z \sim 1$. The galaxies are therefore more frequently warped, and distant warps are brighter and stronger. The rate of the evolution is consistent with the increase of galaxy interactions and mergers (Le Févre et al. 2000, Reshetnikov 2000), which tends to suggest that the source of warping is precisely tidal interaction. Schwarzkopf & Dettmar (2001) estimate that tidal perturbations generate the strongest warps.

As one can find from Table 1, the mean projected starting point of the stellar warps we detected is $\langle R_{warp} \rangle$=3.7±1.3 kpc or, expressed in exponential scalelengths, $1.4 \pm 0.3\,h$. According to de Grijs (1997), the same value for local spirals is $2.1 \pm 1.0\,h$.

No coherence in the orientation of warps was found. This is not surprising, taking into account the large distances involved, of the order of gigaparsecs. Galaxies with close redshifts were too few to be of any consequence. This phenomenon cannot be excluded, however (Battaner et al. 1991, Zurita & Battaner 1997).

4. Discussion and conclusions

The result of the present statistical study is that warps were very frequent in the past, and they were of larger amplitude. One obvious interpretation comes from galaxy interactions that were much more frequent, since they represent an efficient trigger of warps. Indeed the frequency of galaxy pairs and the frequency of mergers is observed to increase as a high power of time, or in $(1+z)^m$, with $m = 3 - 4$ (Le Févre et al. 2000). This is also observed in the fraction of perturbed and distorted galaxies, for instance in the frequency of tidal tails (Reshetnikov, 2000). However, a much lower rate of mergers or mass accretion was observed for bright and massive galaxies by Carlberg et al. (2000). This might be related to the fact that the spheroids or bulge-dominated galaxies appear later in redshift, at the expense of disk-dominated and irregular galaxies (Kajisawa & Yamada, 2001). This is expected in a hierarchical cosmological scenario, where galaxies are formed by successive mergers. Galaxies are then more frequent in the past, per comoving volume. Moreover, due to expansion, the density of galaxies was larger (increasing as $(1 + z)^3$ for a homogeneous universe). On the other hand, galaxies were smaller, and the warps appear to begin at a smaller radius. At this distance from the center, the differential precessing rates of orbits is shorter, and the life-time of warps should be smaller (roughly proportional to R_{warp}, for flat rotation curves).

Another possible triggering of warps is the action of an intergalactic magnetic fields. In a highly conductive homogeneous universe, magnetic fields increase as $(z + 1)^2$ (Battaner & Florido 2001), which means a factor of 4 at $z = 1$. However, at $z = 1$, with a highly inhomogeneous universe the condition of frozen-in magnetic field lines should better describe the evolution of magnetic fields. We adopt $B\rho^{-2/3}$=constant. Then, for a present-day cluster overdensity of 10, the magnetic field strength should be $2^{2/3} = 1.6$ larger than today. Magnetic fields larger by a factor 1.6-4 also constitute a potential explanation of the increased warping amplitude in the past.

The infall of dark and visible matter either on halos (Ostriker & Binney 1989) or on disks, producing reorientation of the galactic angular momentum, should have been greater in the past. Therefore the infall mechanism could also be a dominant effect to explain the high rate of $z \sim 1$ warps.

Finally, we would like to stress that our results are obtained for very small regions of the celestial sphere. Moreover, the statistics are based on small numbers. Therefore, further extended studies of distant edge-on galaxies are highly needed to develop our preliminary results.

Acknowledgements. This work was begun while V.R. was visiting Paris, thanks to a one month grant from Paris Observatory.

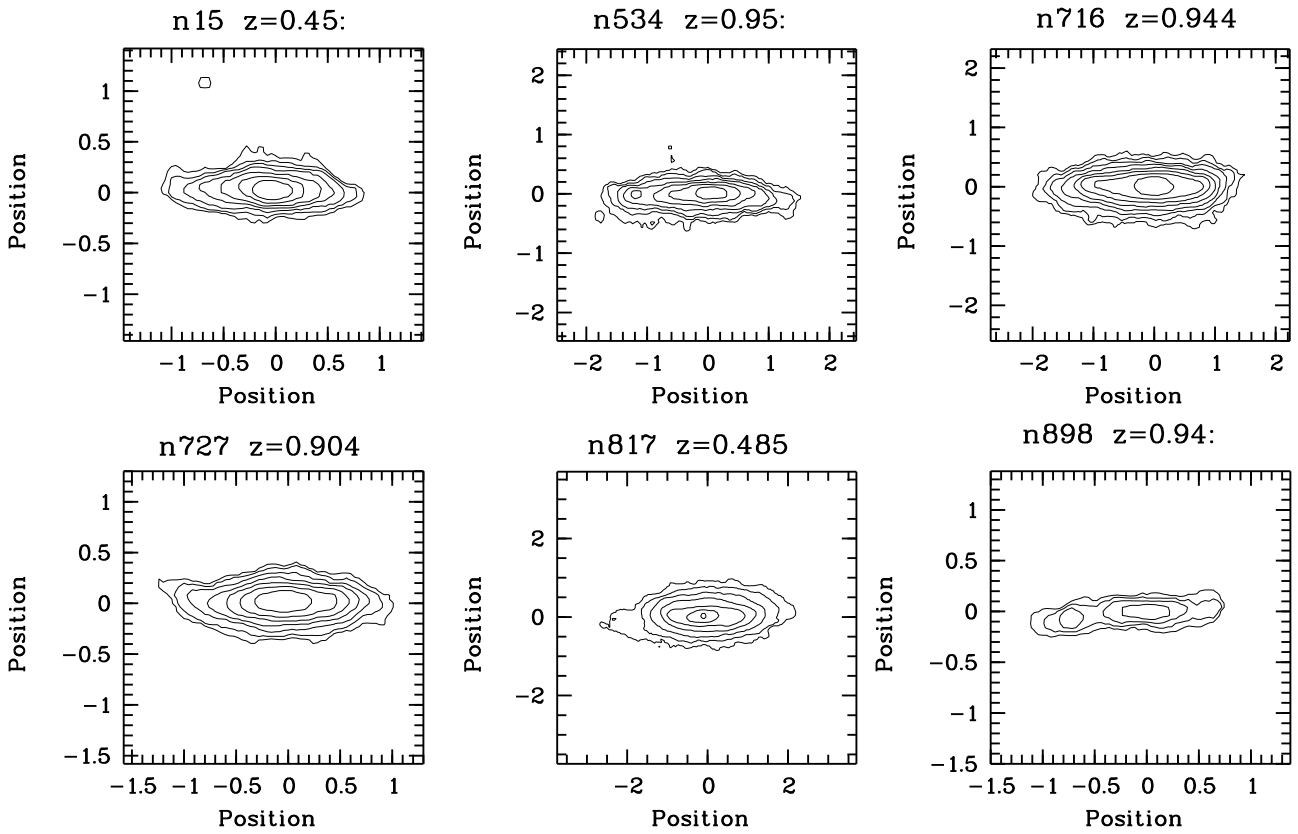

Fig. 6. Contour plots of galaxies with certain or possible warps (see tables 1 and 2). Both axes are in arcseconds (size of 1 pixel of the original fields is $0.''04$). The faintest contour corresponds to $\mu(I_{814}) = 26.0$, isophotes step is $0.^m44$ ($0.^m75$ for n817). Uncertain values of z obtained as the mean of two photometric redshifts (see tables 1 and 2) are marked as (:).

We would like to thank R. de Grijs and A.Guijarro for providing the image of ESO 235-G53 in the B passband.

References

Battaner, E., & Florido, E. 2001, Fundamentals of Cosmic Physics, 21, 1
Battaner, E., Florido, E., & Sánchez-Saavedra, M.L. 1990, A&A, 236, 1
Battaner, E., Garrido, J.L., Sánchez-Saavedra, M.L., & Florido, E. 1991, A&A, 251, 402
Binney, J. 1992, ARAA 30, 51
Binney, J., Jiang, I., & Dutta, S. 1998, MNRAS, 297, 1237
Bosma, A. 1981, AJ, 86, 1825
Briggs, F. H. 1990, ApJ, 352, 15
Carlberg R., Cohen, J. G., Patton, D. R. et al. 2000, ApJ 532, L1
Cohen, J.G., Hogg, D.W., Blandford, R., et al. 2000, ApJ, 538, 29
Davé, R., Hernquist, L., Katz, N., & Weinberg, D. H. 1999, ApJ, 511, 521
de Grijs, R. 1997, Edge-on Disk Galaxies, Thesis, Groningen
Fernández-Soto, A., Lanzetta, K.M., & Yahil, A. 1999, ApJ, 513, 34
Fontana, A., D'Odorico, S., Poli, F., et al. 2000, AJ, 120, 2206
Giavalisco, M., Livio, M., Bohlin, R.C., et al. 1996, AJ, 112, 369
Guthrie, B.N.G. 1992, A&AS, 93, 255
Gwyn, S.D.J. 1999, in Photometric Redshifts and High Redshift Galaxies, Weymann, R., Storrie-Lombardi, L., Sawicki, M., & Brunner, R. eds., San Francisco, 61 [astro-ph/9907336]
Hogg, D.W., Pahre, M.A., Adelberger, K.L., et al. 2000, ApJS, 127, 1
Jiang, I. & Binney, J. 1999, MNRAS, 303, L7
Jiménez-Vicente, J., Porcel, C., Sánchez-Saavedra, M.L., & Battaner, E. 1997, A&SS, 253, 225
Fontana, A., D'Odorico, S., Poli, F., et al. 2000, AJ, 120, 2206
Ferguson, H.C., Dickinson, M., & Williams, R. 2000, ARAA, 38,667
Karachentsev, I.D., & Karachentseva, V.E. 1974, Astron. Zh., 51, 724
Kajisawa M., Yamada T.: 2001, PASJ 53, 833
Le Févre, O., Abraham, R., Lilly, S.J., et al. 2000, MNRAS, 311, 565

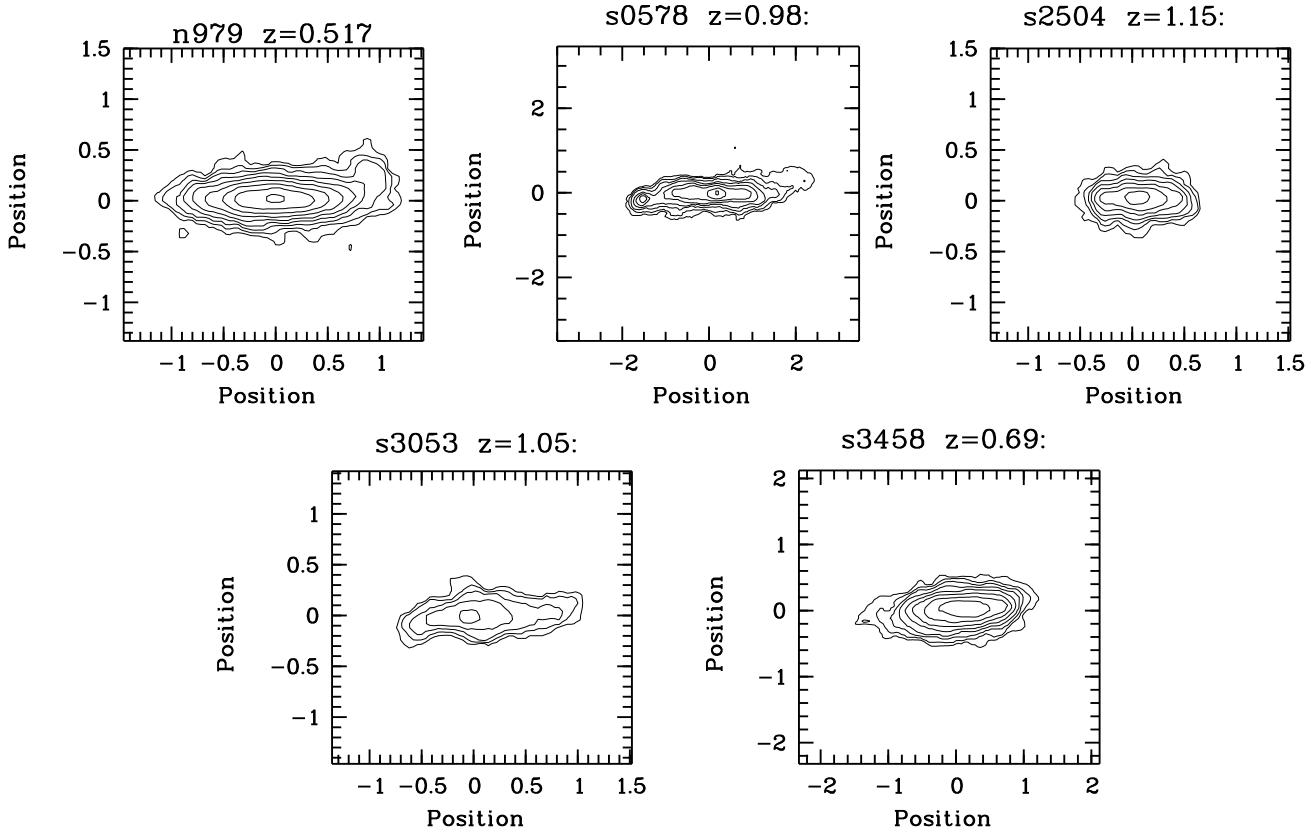

Fig. 7. Contour plots of galaxies with certain or possible warps (continued).

Lilly, S.J., Tresse, L., Hammer, F., et al. 1995, ApJ, 455, 108
Lilly, S., Schade, D., Ellis, R., et al. 1998, ApJ, 500, 75
Nelson, R. W. & Tremaine, S. 1995, MNRAS, 275, 897
Oke, J.B. 1974, ApJS, 27, 21
Ostriker, E.C., & Binney, J.J. 1989, MNRAS, 237, 785
Reshetnikov, V.P. 1995, A&ATr, 8, 31
Reshetnikov, V.P. 2000, A&A, 353, 92
Reshetnikov, V., & Combes, F. 1997, A&A, 324, 80
Reshetnikov, V., & Combes, F. 1998, A&A, 337, 9
Reshetnikov, V., & Combes, F. 1999, A&AS, 138, 101
Sánchez-Saavedra, M. L., Battaner, E., & Florido, E. 1990, MNRAS, 246, 458
Schmidt, M. 1968, ApJ, 151, 393
Schwarzkopf, U., & Dettmar, R.-J. 2000, A&A, 361, 451
Schwarzkopf, U., & Dettmar, R.-J. 2001, A&A, 373, 402
Shang, Z. et al. 1998, ApJ, 504, L23
Thuan, T.H., & Seitzer, P.O. 1979, ApJ, 231, 680
van den Bergh, S., Cohen, J. G., Hogg, D. W., Blandford, R. 2000, AJ 120, 2190
Williams, R.E., Blacker, B., Dickinson, M., et al. 1996, AJ, 112, 1335
Zurita, A., Battaner, E., 1997, A&A 322, 86